Clusters of secretagogin-expressing neurons in the aged human olfactory tract lack terminal differentiation

Johannes Attems[a,1], Alan Alpar[b,c,1], Lauren Spence[b], Shane McParland[a], Mathias Heikenwalder[d], Mathias Uhlén[e], Heikki Tanila[f], Tomas G. M. Hökfelt[g,2], and Tibor Harkany[b,c,2]

[a]Institute for Ageing and Health, Newcastle University, Newcastle upon Tyne NE4 5PL, United Kingdom; [b]European Neuroscience Institute at Aberdeen, University of Aberdeen, Aberdeen AB25 2ZD, United Kingdom; [c]Division of Molecular Neurobiology, Department of Medical Biochemistry and Biophysics, and [g]Department of Neuroscience, Karolinska Institutet, SE-17177 Stockholm, Sweden; [d]Institute of Virology, Technische Universität/Helmholtz Zentrum München, D-81675 Munich, Germany; [e]Science for Life Laboratory, Royal Institute of Technology, SE-17121 Stockholm, Sweden; and [f]Department of Neurology, Kuopio University Hospital and A. I. Virtanen Institute, University of Eastern Finland, FI-70211, Kuopio, Finland

Contributed by Tomas G. M. Hökfelt, March 6, 2012 (sent for review November 10, 2011)

Expanding the repertoire of molecularly diverse neurons in the human nervous system is paramount to characterizing the neuronal networks that underpin sensory processing. Defining neuronal identities is particularly timely in the human olfactory system, whose structural differences from nonprimate macrosmatic species have recently gained momentum. Here, we identify clusters of bipolar neurons in a previously unknown outer "shell" domain of the human olfactory tract, which express secretagogin, a cytosolic Ca^{2+} binding protein. These "shell" neurons are wired into the olfactory circuitry because they can receive mixed synaptic inputs. Unexpectedly, secretagogin is often coexpressed with polysialylated–neural cell adhesion molecule, β-III-tubulin, and calretinin, suggesting that these neurons represent a cell pool that might have escaped terminal differentiation into the olfactory circuitry. We hypothesized that secretagogin-containing "shell" cells may be eliminated from the olfactory axis under neurodegenerative conditions. Indeed, the density, but not the morphological or neurochemical integrity, of secretagogin-positive neurons selectively decreases in the olfactory tract in Alzheimer's disease. In conclusion, secretagogin identifies a previously undescribed cell pool whose cytoarchitectonic arrangements and synaptic connectivity are poised to modulate olfactory processing in humans.

calcium signaling | neurodegeneration | neurogenesis | relay circuit | tau

Olfaction is an ancient sense of vertebrates pivotal for the individual's environmental adaptation, competitiveness, and survival. The olfactory system is the phylogenetically oldest part of the forebrain, with its proportion to the total brain volume progressively decreasing from rodents to humans (1–3). Rodents maintain and continuously refine their olfactory system by adding new neurons throughout life to olfactory glomeruli via the rostral migratory stream (RMS) (4, 5). The microsmatic character of humans is frequently associated with the reduced size of the rhinencephalon. The lack of rodent-like lifelong plasticity in the human olfactory circuitry may be related, at least in part, to the neonatal disappearance of continued chain migration of immature neurons in the human homolog of the RMS (6–10).

Mitral and tufted cells, output neurons of the main olfactory bulb (1), send olfactory information to interrelated allo- or neocortical areas via their axons coursing in the olfactory tract. The olfactory tract is particularly well formed and elongated in humans (and primates; ref. 11) and is believed to be neuron-free except from dispersed cells displaced from retrobulbar and prepiriform regions (12).

Ca^{2+} binding and sensor proteins sculpt fundamental nervous system functions and are used as selective markers for neuronal subpopulations (13). Secretagogin is a recently cloned Ca^{2+} binding protein (14) whose Ca^{2+} sensor functions are becoming increasingly appreciated (15). During the analysis of the primate olfactory system, we found secretagogin-positive (secretagogin$^+$) neurons in the RMS and olfactory bulb (16). Therefore, we hypothesized that secretagogin may reveal previously undescribed cellular identities and cytoarchitectural arrangements in the human olfactory axis. Here, we report the existence of a neuron-rich cellular niche in the outer "shell" domain of the human olfactory tract, containing bipolar secretagogin$^+$ cells neurochemically resembling deep-layer and periglomerular olfactory interneurons (17) and synaptically integrated into the olfactory circuitry. Clustered "shell" cells retain molecular markers of immature neuronal identity in a descending gradient toward the olfactory bulb.

Olfactory dysfunction is a prevalent premonitory sign of Alzheimer's disease (AD) due to damage to olfactory centers or regions interrelated with the olfactory pathway (18). We show the selective decline of secretagogin$^+$ shell cells in the olfactory tract in AD. In contrast, secretagogin$^+$ periglomerular neurons survive and remain devoid of amyloid β (Aβ) or tau pathology. Overall, we define a unique neuronal subtype in the human olfactory system whose loss can be implicated in impaired olfactory information processing during aging and under neurodegenerative conditions.

Results and Discussion

Secretagogin Identifies Bipolar Cells in the Human Olfactory Tract. We have recently shown secretagogin$^+$ periglomerular interneurons in the olfactory bulb of the gray mouse lemur (*Microcebus murinus, Primates*) (16). However, whether secretagogin is expressed in the human olfactory system remains unknown. Here, we address secretagogin's distribution and the identity of cells in the human olfactory tract and bulb (Table S1), rostral from the olfactory trigone and excluding presumed proliferative zones (Fig. 1*A*), by using affinity-purified polyclonal antibodies whose specificity has been established (16) (Table S2).

Secretagogin immunoreactivity was localized to oval-shaped cells with a somatic diameter of 8–15 μm and distributed along the olfactory trigone (Fig. 1*B*), as well as the entire length of the olfactory tract (Figs. 1 *C*–C_4 and 2 *A* and *B*). Clusters of four to five secretagogin$^+$ cells were often observed. This cytoarchitectural arrangement of secretagogin$^+$ cells did not resemble the dense continuum of chain-migrating neuroblasts in the rodent or primate

Author contributions: J.A., A.A., T.G.M.H., and T.H. designed research; J.A., A.A., L.S., S.M., M.H., and T.H. performed research; M.U. and H.T. contributed new reagents/analytic tools; J.A., A.A., L.S., S.M., M.H., H.T., and T.H. analyzed data; and A.A., L.S., T.G.M.H., and T.H. wrote the paper.

The authors declare no conflict of interest.

[1]J.A. and A.A. contributed equally to this work.

[2]To whom correspondence may be addressed. E-mail: tomas.hokfelt@ki.se or tibor.harkany@ki.se.

This article contains supporting information online at www.pnas.org/lookup/suppl/doi:10.1073/pnas.1203843109/-/DCSupplemental.

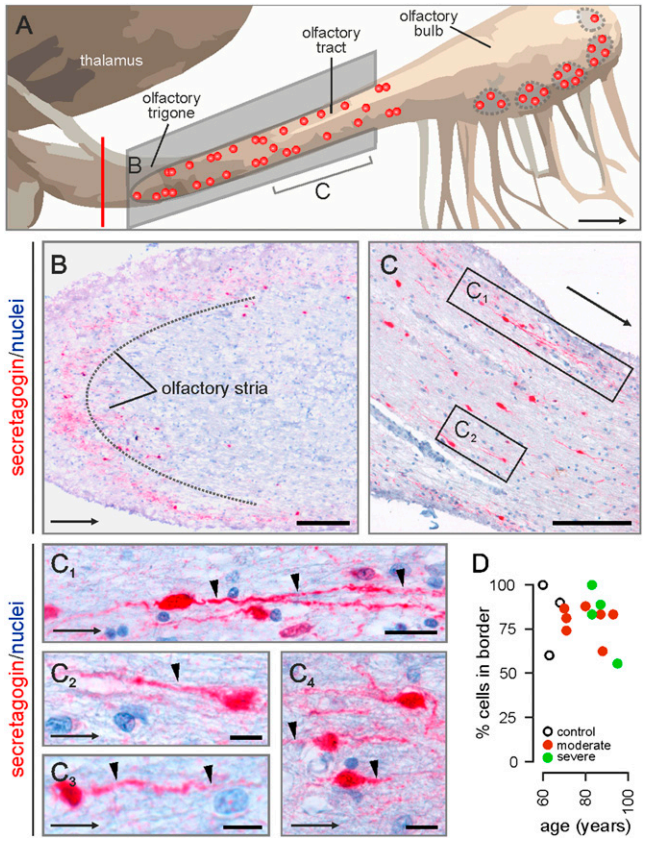

Fig. 1. Secretagogin in the human olfactory tract and bulb. (*A*) Schematic outline of the human olfactory system. Vertical red line denotes the approximate tissue cutoff at the level of the olfactory trigone. Red circles indicate the positions of identified secretagogin$^+$ cells. (*B* and *C*) Immunostained perikarya and processes load the olfactory trigone (*B*), tract (*C*), and bulb. (*B*) Secretagogin$^+$ cells along the opposite margins of the olfactory stria. (*C*) Bipolar neurons align the human olfactory tract. Processes (arrowheads in C_1–C_4) occasionally ramify (C_1). (*D*) Independent of age or Alzheimer's severity, secretagogin$^+$ neurons invariably accumulate in the outer shell domain (100–300 μm from the surface) of the olfactory tract. Arrows indicate direction toward the olfactory bulb. [Scale bars: 250 μm (*B* and *C*), 20 μm (C_1), and 10 μm (C_2–C_4).]

RMS (4, 19). Secretagogin$^+$ cells exhibited bipolar morphology (Fig. 1*C*) with a process emanating at the cell surface facing the olfactory bulb. Although we cannot exclude the occasional pruning of peripheral dendrites during histochemistry, this forward-facing process typically ramified into two or three branches of equivalent length (Fig. 1C_1). Nonbipolar phenotypes were only observed in the proximal part of the olfactory tract (Fig. 2*B*). Secretagogin filled the entire cytoplasm, including processes of >100 μm in length. Because transversal sections of the olfactory striae showed uninterrupted secretagogin immunoreactivity (Fig. 1*B*), we propose that, besides aligning longitudinally along the opposite margins of the olfactory tract (Fig. 1 *B* and *C*), secretagogin$^+$ cells populate an onion skin-like shell proximal to the superficial (outer) surface of the olfactory tract (Fig. 2*A*). Secretagogin$^+$ cells invariably populated the outer region of the olfactory tract, irrespective of the lifespan (ranging from 60 to 95 y) of the cases studied (Fig. 1*D*). Although a bipolar neuronal phenotype in the olfactory system could allude to migratory behaviors, an equally appealing hypothesis is that intercalated mitral cell axons force the morphological adaptation of secretagogin$^+$ cells. The latter notion is supported by the association of Ca^{2+}-binding protein-containing bipolar neurons to axonal tracts in the corpus callosum (20) and anterior medullary velum (21).

Secretagogin$^+$ Bipolar Cells Receive Synaptic Input. Secretagogin$^+$ cells must receive synaptic inputs if they are integrated in the olfactory circuitry. Typically, relay cells receive dense afferentation on their somatodendritic compartments (22). We found secretagogin$^+$ cells expressing MAP-2, a somatodendritic marker of neurons (Fig. 2 *D* and D_1), and being apposed by presynapses (Fig. 2*B*) immunoreactive for synaptobrevin-2 (Fig. 2 *E*–E_2), synaptophysin (Fig. 2 *F* and F_1), or glutamic acid decarboxylase [65/67-kDa isoforms (GAD65/67); Fig. 2 *G* and G_1].

Next, we tested whether secretagogin$^+$ neurons were restricted to the human olfactory tract or might have also been present in an analogous structure of primates by studying the gray mouse lemur (Fig. S1 *A* and *B*). We identified secretagogin$^+$ bipolar neurons along the shaft of the lemur's olfactory tract (Fig. S1*B*), in which the neurochemical attributes and synaptic innervation patterns (Fig. 2 *H* and *I* and Fig. S1 *D*–*F*) were reminiscent of those of human secretagogin$^+$ neurons. Because shell cells received both excitatory [vesicular glutamate transporter 1$^+$ (VGLUT1$^+$); Fig. 2 *J* and J_1) and inhibitory (GAD65/67$^+$; Fig. 2 *K*–K_2) afferents and expressed corresponding postsynaptic receptor subunits ($GABA_A$Rα1; Fig. 2K_2), we suggest that these cells can be synaptically wired into the olfactory circuitry.

Secretagogin$^+$ Cells Express Neuronal Plasticity Markers. The scarce innervation of secretagogin$^+$ cells together with their lack of mature neuronal markers [NeuN (23) or system A amino acid transporter 2 (SAT2), preferentially labeling excitatory neurons (24); Fig. 2*L* and Fig. S2, but see Fig. 5*A*] prompted us to test whether secretagogin$^+$ cells represent a cell cohort that had retained immature characteristics (4, 7, 25).

Doublecortin immunoreactivity could not be detected unambiguously in the adult human olfactory system. Where noticeable, as in primates (16), secretagogin$^+$ neuroblasts lacked doublecortin expression. We found unexpectedly high levels of polysialylated–neural cell adhesion molecule (PSA-NCAM), a widely accepted neuronal and structural plasticity marker (8, 25), in the olfactory tract (Fig. 3*A*) and bulb (Fig. S3 *A* and A_1) of aged humans. We demonstrated that PSA-NCAM$^+$ shell cells frequently coexpressed secretagogin (Fig. 3 *A*–A_4). Secretagogin coexisted with calretinin (CR), another neuron-specific Ca^{2+} binding protein (13, 26), in shell cells, particularly in superficial cell assemblies near the outer margin of the olfactory tract (Fig. 3 *B* and *C*). We observed a gradual decrease in the density of PSA-NCAM$^+$/secretagogin$^+$ or CR$^+$/secretagogin$^+$ cells, uniformly bipolar in morphology (Fig. 2*B*), in the olfactory tract, which had tailed off toward the olfactory bulb (Fig. 2*C*). Irrespective of the age of the study subjects, secretagogin$^+$ neurons in the olfactory tract exhibited low to moderate levels of β-III-tubulin (TUJ1) immunoreactivity (Fig. 3 *D1* and D_2). The lack of glial fibrillary acidic protein (GFAP) expression (Fig. 3 *E*–E_2) in secretagogin$^+$ cells in the human olfactory system reinforces our hypothesis that this cell population is of neuronal origin. The presence of PSA-NCAM$^+$/secretagogin$^+$ neurons in the adult primate olfactory tract (Fig. S1*C*) supports the notion that PSA-NCAM expression is unlikely to represent a cellular response to injury or neurodegeneration. Overall, PSA-NCAM, CR, and TUJ1 expression by secretagogin$^+$ cells suggests that these may retain some characteristics of immature neurons but are synaptically connected in the olfactory system.

Secretagogin Labels Periglomerular Cells in the Human Olfactory Bulb. Recently, we identified secretagogin as a marker of periglomerular and deep-layer olfactory interneurons in the mouse and monkey (16). Therefore, we hypothesized that secretagogin may be expressed along the entire human olfactory axis. Indeed, a dense plexus of secretagogin$^+$ neurons was seen throughout the human olfactory bulb (Fig. S3*A*). Secretagogin$^+$ interneurons were often encountered in plexiform, granular, and, to a lesser extent, mitral cell layers (Fig. 5 *A*–*C* and Fig. S3*B*).

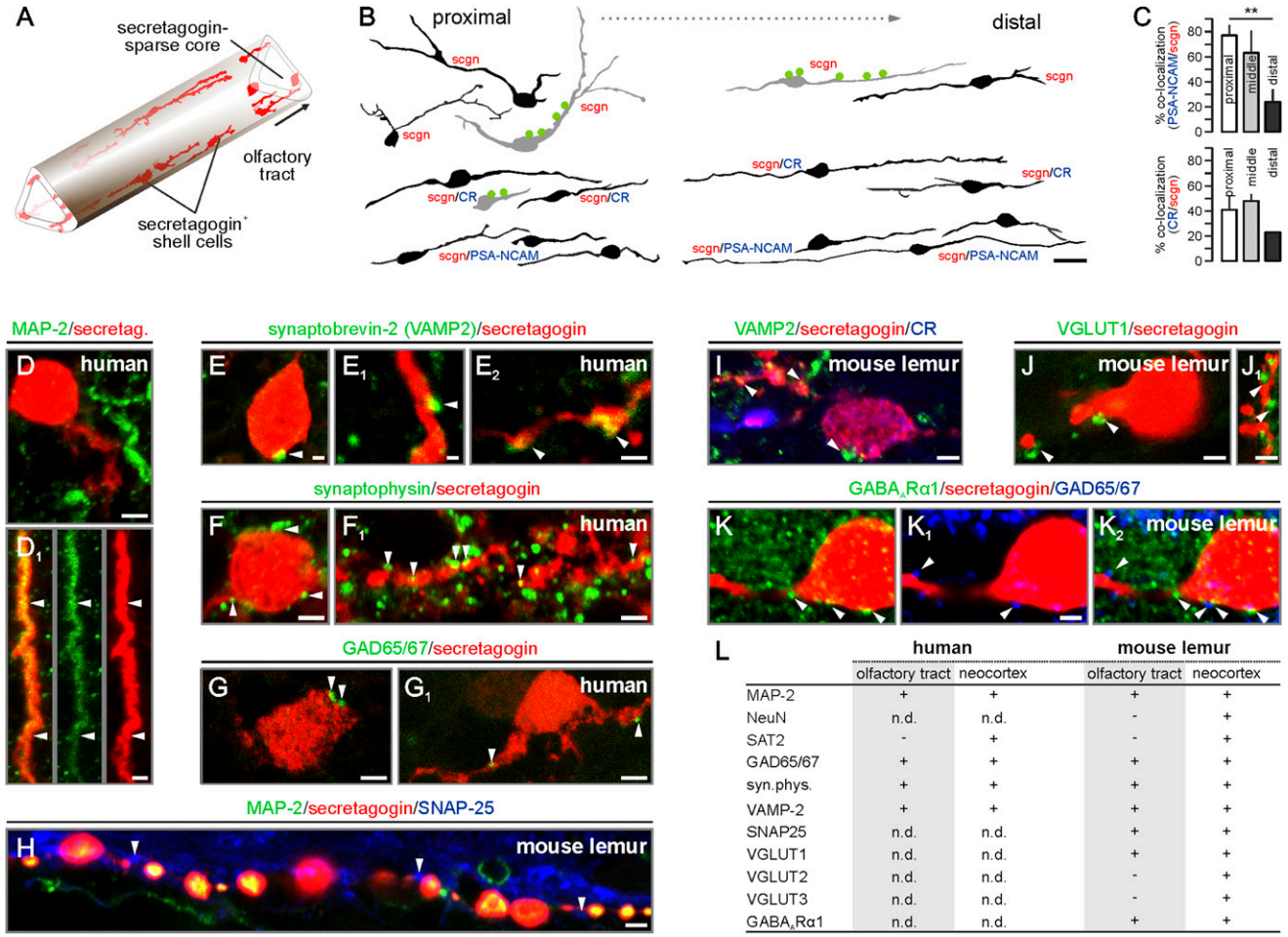

L

	human		mouse lemur	
	olfactory tract	neocortex	olfactory tract	neocortex
MAP-2	+	+	+	+
NeuN	n.d.	n.d.	-	+
SAT2	-	+	-	+
GAD65/67	+	+	+	+
syn.phys.	+	+	+	+
VAMP-2	+	+	+	+
SNAP25	n.d.	n.d.	+	+
VGLUT1	n.d.	n.d.	+	+
VGLUT2	n.d.	n.d.	-	+
VGLUT3	n.d.	n.d.	-	+
GABAARα1	n.d.	n.d.	+	+

Fig. 2. Secretagogin$^+$ neurons of the olfactory tract synaptically integrate into the olfactory circuitry. (*A*) Secretagogin$^+$ bipolar shell cells populate the margins of the human olfactory tract. (*B*) Secretagogin$^+$ cells are predominantly bipolar, except a subset of multipolar calretinin (CR)$^-$/PSA-NCAM$^-$ shell cells at locations proximal to the trigone. Somatodendritic afferents are in green. (*C*) The percentage of secretagogin$^+$/CR$^+$ and secretagogin$^+$/PSA-NCAM$^+$ neurons declines toward the distal olfactory tract. $^{**}P < 0.01$. (*D* and D_1) Dendritic (arrowheads), but not somatic MAP-2, immunoreactivity was seen in secretagogin$^+$ neurons. (*E–H*) Synaptobrevin$^+$ (*E–*E_2), synaptophysin$^+$ (*F* and F_1), or GAD65/67$^+$ (*G* and G_1) profiles (arrowheads) on secretagogin$^+$ somata and dendrites. (*H–K*) Similar to the human olfactory tract, SNAP25$^+$ (*H*), synaptobrevin-2$^+$ (*I*), VGLUT1$^+$ (*J* and J_1), or GAD65/67$^+$ (*K–*K_2) boutons contact secretagogin$^+$ somata or processes in the mouse lemur olfactory tract. Note that postsynaptic GABA$_A$Rα1 subunits (31) appose GAD65/67$^+$ afferents (K_2). (*L*) Markers of cellular identity and afferent synapses on secretagogin$^+$ neurons (n.d., nondetectable due to e.g., epitope mismatch). [Scale bars: 10 μm (*B*), 3 μm (*D*, E_2, *F*, *G*, and G_1), 2 μm (D_1, F_1, *H*, *I*, I_1, *J*, *K*, K_1, and K_2), and 1 μm (*E* and E_1).]

Loss of Secretagogin Expression in the Olfactory Tract in AD. The temporally precise and coordinated activity of periglomerular interneurons participates in the continuous refinement of olfactory inputs (5, 19). One of the early clinical signs of AD is perturbed olfactory processing (27). Therefore, we asked whether secretagogin$^+$ olfactory neurons might be affected or lost under conditions of AD pathology. We used a patient cohort of 16 AD cases and 4 age-matched controls (Table S1). The density of AT8$^+$ hyperphosphorylated tau-bearing olfactory neurons exhibited a significant positive correlation with advancing Braak stages ($\rho = 0.876$, $P < 0.01$; Table S1).

Secretagogin$^+$ cells contained hyperphosphorylated tau in the olfactory tract (Fig. 4 *A–*A_1″). Their number significantly declined with age (Fig. 4*B*). The loss of shell cells became accentuated upon binning our patient material as per AD staging ($P < 0.05$ vs. control; Fig. 4B_1). In contrast, the pattern of secretagogin immunoreactivity in the perikarya or dendrites in the periglomerular layer of the olfactory bulb (Fig. 5 *B* and *C*) did not show significant changes in AD cases relative to controls (Fig. 5*C*). Both the total number of cells (Fig. 5C_1) and the percentage of secretagogin$^+$ neurons in individual olfactory glomeruli (Fig. 5C_2) remained unperturbed with no correlation to age (Fig. 5C_3) or to one another (Fig. 5C_4). These data suggest that secretagogin$^+$ neurons in the olfactory tract focally and selectively succumb to neurofibrillary pathology in AD.

Next, we tested whether secretagogin$^+$ neurons were affected by AD-related cytoskeletal modifications. Although dendritic fields within olfactory glomeruli exhibited AT8 immunoreactivity (likely corresponding to the primary dendritic tuft of mitral cells and/or primary olfactory afferents), secretagogin$^+$ periglomerular interneurons did not accumulate hyperphosphorylated tau (Fig. 5*D*). The periglomerular layer was devoid of extracellular Aβ plaques in all cases (27) (Fig. 5 *E* and E_1), excluding the study of a direct relationship between Aβ toxicity and secretagogin expression in the human olfactory system.

The olfactory bulb harbors neurochemically distinct subsets of interneurons (1, 17). The expression of CR, parvalbumin, and calbindin-D28k by olfactory interneurons is used to subclassify these cells (17). Rodent and primate studies revealed secretagogin's propensity to coexist with CR, but less so with parvalbumin or calbindin-D28k (16). Here, we assessed whether secretagogin$^+$ interneurons retained their ability to coexpress CR in AD. By

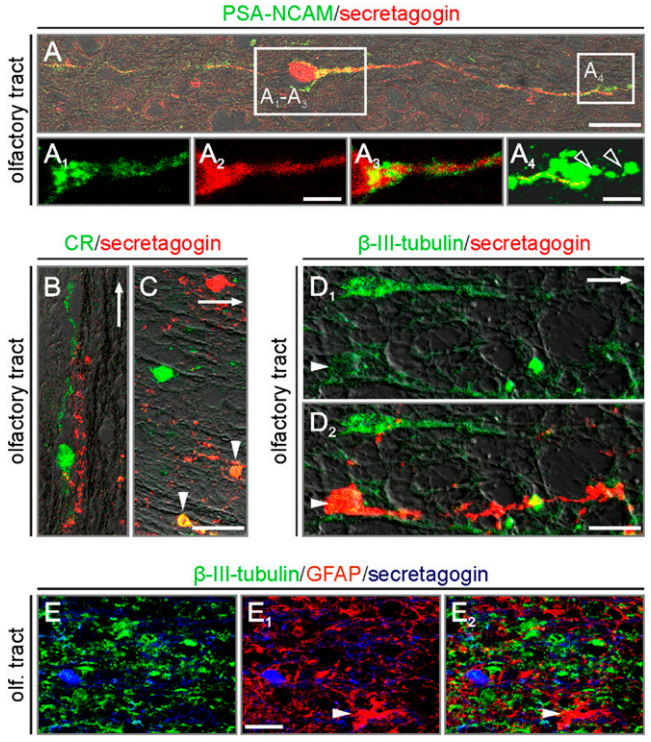

Fig. 3. Secretagogin identifies bipolar cells with a makeup of immature neurons. (*A*) PSA-NCAM enwraps secretagogin$^+$ bipolar cells (note that secretagogin is cytosolic). Open rectangles pinpoint the positions of A_1–A_3 *Insets* and a terminal specialization, likely growth cone (A_4, open arrowheads). (*B*) CR$^+$ and secretagogin$^+$ processes run in parallel. (*C*) Secretagogin colocalizes with CR (arrowheads). (D_1 and D_2) β-III-tubulin coexists in secretagogin$^+$ shell cells (arrowheads). Arrows in *B*–*D* and D_1 point toward the olfactory bulb. (E–E_2) Secretagogin$^+$ neurons lack GFAP (arrowhead points to glial cell) immunoreactivity. [Scale bars: 20 μm (*B* and *C*), 10 μm (*A* and D_2), 7 μm (E_1), 5 μm (A_2), and 2 μm (A_4).]

determining the probability of colocalization of these Ca^{2+} binding proteins on sufficiently large and randomized cell populations in the glomerular, external plexiform, and granular cell layers (Fig. 5*F* and Fig. S3*B*), we found a transient (albeit nonsignificant) increase in secretagogin/CR colocalization in moderate AD. The density of secretagogin$^+$/CR$^+$ interneurons remained unchanged in severe AD relative to controls (Fig. 5*F* and Fig. S3*C*). Parvalbumin$^+$ interneurons were devoid of secretagogin expression in either AD or control cases. We conclude that the identity of secretagogin$^+$ cells and their laminar distribution pattern in the olfactory bulb remain unaffected in AD. In view of the lack of Aβ deposits in the human olfactory glomerular layer, the analysis of a transgenic mouse model presenting Aβ-induced olfactory impairments (28) is warranted.

Secretagogin Expression in Mice with AD-Like Pathology. APdE9 mice are characterized by robust and progressive amyloid plaque deposition in the olfactory bulb (Fig. S4 *A*, *B*, and B_1). Because mice do not have an equivalent to the primate olfactory tract, we focused on Aβ-laden forebrain territories containing undifferentiated secretagogin$^+$ neuroblasts and/or terminally differentiated neurons to test whether Aβ can induce the loss of secretagogin$^+$ olfactory neurons.

We show that transgene-driven Aβ accumulation in APdE9 mice failed to impact the laminar distribution or cellular integrity of secretagogin$^+$ neurons in the mouse olfactory bulb (Fig. 5 G–G_2) or indusium griseum (Fig. S4 D_1 and D_1'). High-resolution confocal microscopy revealed chain-migrating secretagogin$^+$ neuroblasts in the RMS, populating the olfactory bulb in both APdE9 mice and wild-type controls (Fig. S4 C_1 and D_2). The density of secretagogin$^+$ neuroblasts entering the olfactory bulb did not differ between APdE9 mice and wild-type littermates [8.4 ± 1.3 (APdE9) vs. 6.6 ± 0.6 (wild-type) cells per 10^4 μm^2; $P > 0.1$]. Despite the severe Aβ burden, neither the morphological phenotype nor the packing density of secretagogin$^+$ periglomerular neurons was qualitatively different in either the accessory (Fig. S4 C_3 and D_3) or the main olfactory bulb (Fig. S4 C_2 and D_4). Our experimental data suggest that secretagogin expression is unaffected by Aβ, because secretagogin$^+$ neuroblasts and neurons remain unaltered both in their contingents and phenotypes, recapitulating histopathological findings in AD. These data raise the possibility that a phylogenetically segregated subset of secretagogin$^+$ neurons is selectively lost during AD, implicating a spatially-confined cellular locus for olfactory impairment in aged humans.

Conclusions

Understanding the neuronal substrates of olfaction, particularly the neuronal subtypes conferring critical network modalities, received limited attention in humans because of the lack of neurochemical cell identity markers allowing the precise mapping of spatial and temporal modifications to the olfactory circuitry. The continued identification of molecularly and morphologically diverse neuronal subtypes in the human olfactory circuitry, like in rodents (29), may be rewarding because it can uncover striking phylogenetic differences (30). Here, we show the existence of spatially segregated neurons expressing secretagogin, as well as a battery of markers nonconventional for differentiated neurons that had integrated into a synaptic circuitry. These shell cells are unique to primates and humans, emphasizing interspecies differences in the cytoarchitectural organization of the olfactory circuitry. Our hypothesis is that secretagogin$^+$ shell cells did not reach their final destination in the olfactory bulb during development, yet synaptically integrated to refine some aspects of olfactory information processing. Their atypical localization in the olfactory tract may render secretagogin$^+$ neurons sensitive to noxious insults during AD, giving rise to a spatially restricted primary locus triggering olfactory impairment as AD progresses. Although secretagogin's cellular function(s) remain unknown, an appealing conjecture is that this Ca^{2+} binding

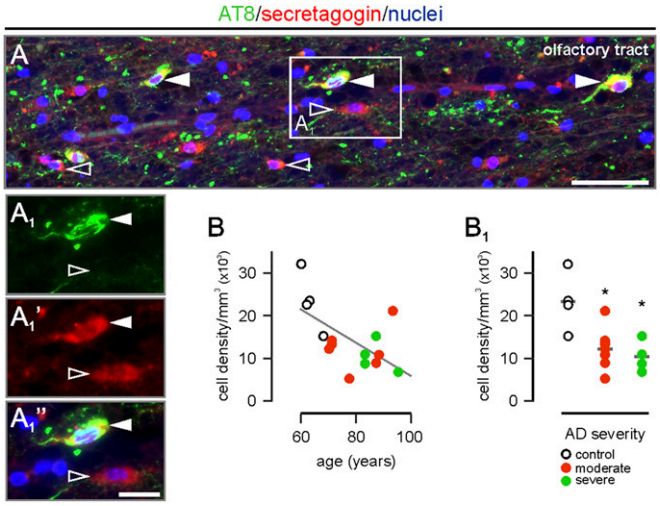

Fig. 4. Secretagogin$^+$ neurons in the olfactory tract are lost in AD. (A–A_1'') Secretagogin$^+$ neurons (open arrowheads) can exhibit neurofibrillary tangle pathology (AT8$^+$) (filled arrowheads) in the human olfactory tract. (*B* and B_1) Age ($R^2 = 0.62$, $P < 0.01$) and Alzheimer's stage-related decline of secretagogin$^+$ shell cells in the olfactory tract. *$P < 0.05$. [Scale bars: 20 μm (*A*) and 10 μm (A_1'').]

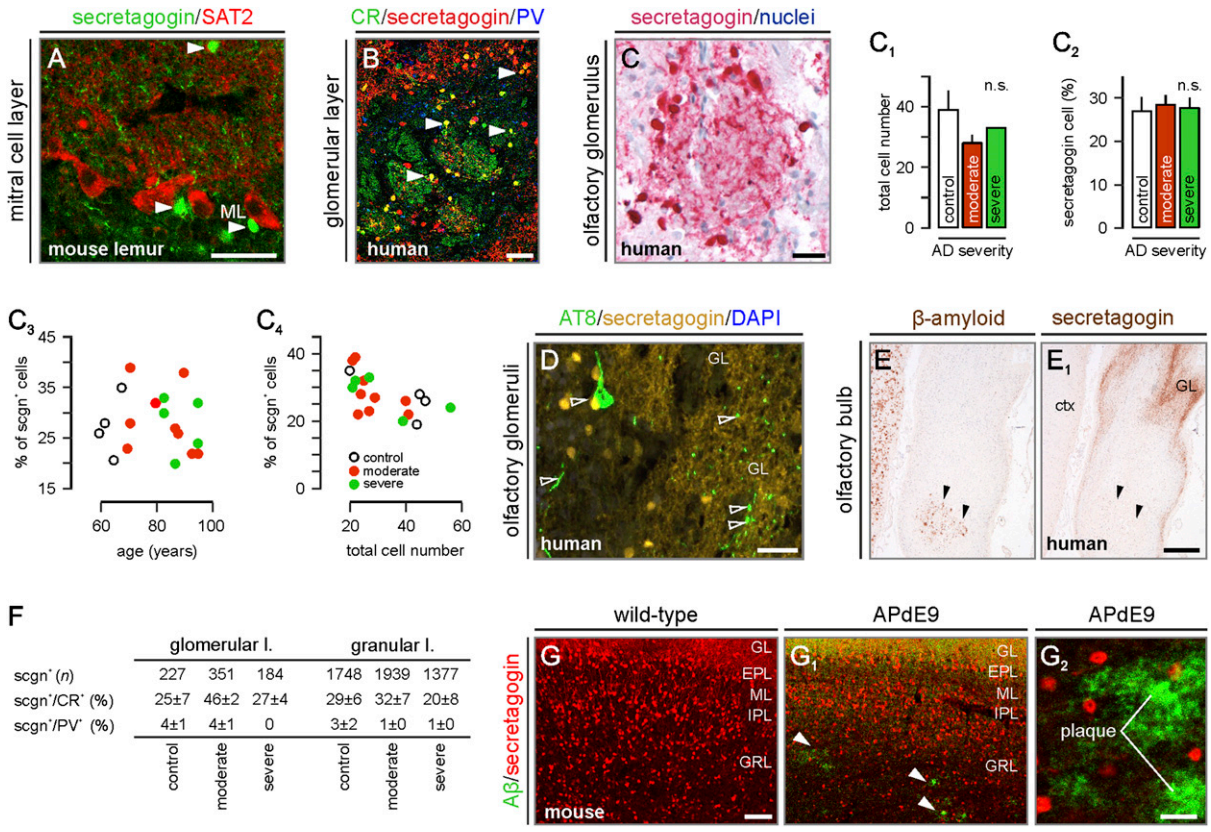

F	glomerular l.			granular l.		
scgn+ (*n*)	227	351	184	1748	1939	1377
scgn+/CR+ (%)	25±7	46±2	27±4	29±6	32±7	20±8
scgn+/PV+ (%)	4±1	4±1	0	3±2	1±0	1±0
	control	moderate	severe	control	moderate	severe

Fig. 5. Secretagogin is retained in the olfactory bulb in AD. (*A*) Secretagogin$^+$ cells, likely interneurons (arrowheads), intermingled with SAT2$^+$ mitral cells in the olfactory bulb. (*B*) Secretagogin and CR often coexist in periglomerular cells (arrowheads). (*C*–*C*$_4$) Quantitative assessment of the total (*C*$_1$) and secretagogin$^+$ cell number (*C*$_2$) in olfactory glomeruli (*C*, Braak VI) in AD (n.s., nonsignificant). Note that the percentage number of secretagogin$^+$ cells per glomerulus fails to correlate with either age (*C*$_3$) or Alzheimer's stage (*C*$_4$). (*D*) Secretagogin$^+$ periglomerular neurons do not contain hyperphosphorylated tau (open arrowheads). (*E* and *E*$_1$) Complementary distribution of β-amyloid (arrowheads) and secretagogin. (*F*) The probability of secretagogin's colocalization with other Ca^{2+} binding proteins. (*G*–*G*$_2$) Unaltered distribution of secretagogin$^+$ neurons in the olfactory bulb despite robust amyloid plaque load (*G*$_2$) in APdE9 mice. GL, glomerular layer; EPL, external plexiform layer; ML, mitral layer; IPL, inner plexiform layer; GRL, granular layer. [Scale bars: 300 μm (*E*$_1$), 140 μm (*G*$_1$), 50 μm (*A*–*C*), 30 μm (*D*), and 25 μm (*G*$_2$).]

protein can contribute to shaping synaptic responsiveness as Ca^{2+} sensor through intermolecular interactions (15).

Materials and Methods

Tissues and Histochemistry. Olfactory bulb and adjoining tract tissues from AD patients and age-matched controls (without clinical signs of neuropsychiatric disease; *n* = 20 cases in total, both sexes) were assigned to this study (Table S1). Experimental protocols on human, primate, and mouse specimens were approved by local authorities (*SI Materials and Methods*).

Immunohistochemistry. Rabbit anti-secretagogin antibodies were generated as described (16). Multiple immunofluorescence histochemistry with mixtures of primary antibodies (Table S2) and Sudan Black B counterstaining to quench tissue autofluorescence were according to published protocols (16) as described in *SI Materials and Methods*.

Imaging. Images of sections processed for chromogenic detection of secretagogin or Aβ were captured by using a Nikon Eclipse 90i microscope equipped with a motorized research microscope system and digital camera head (DS-Qi1Mc; Nikon) and analyzed by using Nikon NIS Elements imaging software. Procedural details of the morphometric analysis are referred to in *SI Materials and Methods*. Single *x*–*y* plane images were captured by laser-scanning microscopy (710LSM; Zeiss).

ACKNOWLEDGMENTS. We thank J. Jankowsky and D. Borchelt for colony founders of the APdE9 strain; F. A. Chauhdry, J.-M. Fritschy, W. Härtig, H. Hioki, H. Martens, and L. Wagner for antibodies; F. Aujard for mouse lemur brains; and J. Mulder for technical contributions during the initial phase of this project. This work was supported by the UK National Institute for Health Research Biomedical Research Centre for Ageing and Age-Related Disease Award (to the Newcastle upon Tyne Hospitals National Health Service Foundation Trust), Medical Research Council UK and Medical Research Council Integrative Toxicology Training Project, Alzheimer's Society, Alzheimer's Research Trust, Dunhill Medical Trust, Scottish Universities Life Science Alliance, European Commission Grant HEALTH-F2-2007-201159, National Institutes of Health Grant DA023214, Swedish Research Council, the Karolinska Institutet, the Marianne and Marcus Wallenberg Foundation, the Helmholtz Foundation, and the European Research Council.

1. Shipley MT, Ennis M, Puche AC (2004) Olfactory system. *The Rat Nervous System*, ed Paxinos G (Academic, San Diego), pp 922–964.
2. Zilles K (1990) Cortex. *The Human Nervous System*, ed Paxinos G (Academic, San Diego), pp 757–802.
3. Rakic P (2009) Evolution of the neocortex: A perspective from developmental biology. *Nat Rev Neurosci* 10:724–735.
4. Lois C, Alvarez-Buylla A (1994) Long-distance neuronal migration in the adult mammalian brain. *Science* 264:1145–1148.
5. Kornack DR, Rakic P (2001) The generation, migration, and differentiation of olfactory neurons in the adult primate brain. *Proc Natl Acad Sci USA* 98:4752–4757.
6. Sanai N, et al. (2004) Unique astrocyte ribbon in adult human brain contains neural stem cells but lacks chain migration. *Nature* 427:740–744.
7. Curtis MA, et al. (2007) Human neuroblasts migrate to the olfactory bulb via a lateral ventricular extension. *Science* 315:1243–1249.
8. Wang C, et al. (2011) Identification and characterization of neuroblasts in the subventricular zone and rostral migratory stream of the adult human brain. *Cell Res* 21: 1534–1550.
9. Sanai N, et al. (2011) Corridors of migrating neurons in the human brain and their decline during infancy. *Nature* 478:382–386.
10. Arellano JI, Rakic P (2011) Neuroscience: Gone with the wean. *Nature* 478:333–334.

11. Carmichael ST, Clugnet MC, Price JL (1994) Central olfactory connections in the macaque monkey. *J Comp Neurol* 346:403–434.
12. Kopsch F, Rauber AA (1940) *Lehrbuch und Atlas der Anatomie des Menschen* (Thieme, Stuttgart).
13. Andressen C, Blümcke I, Celio MR (1993) Calcium-binding proteins: Selective markers of nerve cells. *Cell Tissue Res* 271:181–208.
14. Wagner L, et al. (2000) Cloning and expression of secretagogin, a novel neuroendocrine- and pancreatic islet of Langerhans-specific Ca^{2+}-binding protein. *J Biol Chem* 275:24740–24751.
15. Rogstam A, et al. (2007) Binding of calcium ions and SNAP-25 to the hexa EF-hand protein secretagogin. *Biochem J* 401:353–363.
16. Mulder J, et al. (2009) Secretagogin is a Ca^{2+}-binding protein specifying subpopulations of telencephalic neurons. *Proc Natl Acad Sci USA* 106:22492–22497.
17. Kosaka T, Kosaka K (2010) Heterogeneity of calbindin-containing neurons in the mouse main olfactory bulb: I. General description. *Neurosci Res* 67:275–292.
18. Galvan V, Bredesen DE (2007) Neurogenesis in the adult brain: Implications for Alzheimer's disease. *CNS Neurol Disord Drug Targets* 6:303–310.
19. Carleton A, Petreanu LT, Lansford R, Alvarez-Buylla A, Lledo PM (2003) Becoming a new neuron in the adult olfactory bulb. *Nat Neurosci* 6:507–518.
20. Riederer BM, Berbel P, Innocenti GM (2004) Neurons in the corpus callosum of the cat during postnatal development. *Eur J Neurosci* 19:2039–2046.
21. Ibrahim M, Menoud PA, Celio MR (2000) Neurones in the adult rat anterior medullary velum. *J Comp Neurol* 419:122–134.
22. Madarász M, Tömböl T, Hajdu F, Somogyi G (1983) Quantitative histological study on the thalamic ventro-basal complex of the cat. Numerical aspects of the transfer from medial lemniscal fibers to cortical relay. *Anat Embryol (Berl)* 166: 291–306.
23. Mullen RJ, Buck CR, Smith AM (1992) NeuN, a neuronal specific nuclear protein in vertebrates. *Development* 116:201–211.
24. Jenstad M, et al. (2009) System A transporter SAT2 mediates replenishment of dendritic glutamate pools controlling retrograde signaling by glutamate. *Cereb Cortex* 19:1092–1106.
25. Lois C, Alvarez-Buylla A (1993) Proliferating subventricular zone cells in the adult mammalian forebrain can differentiate into neurons and glia. *Proc Natl Acad Sci USA* 90:2074–2077.
26. Hof PR, Nimchinsky EA, Celio MR, Bouras C, Morrison JH (1993) Calretinin-immunoreactive neocortical interneurons are unaffected in Alzheimer's disease. *Neurosci Lett* 152:145–148.
27. Jellinger KA, Attems J (2005) Alzheimer pathology in the olfactory bulb. *Neuropathol Appl Neurobiol* 31:203.
28. Wesson DW, Levy E, Nixon RA, Wilson DA (2010) Olfactory dysfunction correlates with amyloid-beta burden in an Alzheimer's disease mouse model. *J Neurosci* 30:505–514.
29. Paredes RG, Larriva-Sahd J (2010) Medullary neurons in the core white matter of the olfactory bulb: A new cell type. *Cell Tissue Res* 339:281–295.
30. Bystron I, Blakemore C, Rakic P (2008) Development of the human cerebral cortex: Boulder Committee revisited. *Nat Rev Neurosci* 9:110–122.
31. Fritschy JM, et al. (1992) Five subtypes of type A gamma-aminobutyric acid receptors identified in neurons by double and triple immunofluorescence staining with subunit-specific antibodies. *Proc Natl Acad Sci USA* 89:6726–6730.